

Deuteron Stripping by Heavy Nuclei*

W. D. BARFIELD, B. M. BACON, AND L. C. BIEDENHARN†
 Los Alamos Scientific Laboratory, Los Alamos, New Mexico
 (Received September 22, 1961)

Theoretical angular distributions for the proton groups following bombardment of Pb²⁰⁶ and Bi²⁰⁹ by deuterons with energies less than 10 Mev are compared with experimental measurements of Stokes. Both theoretical and experimental angular distributions show peaking in the backwards direction, characteristic where Coulomb effects dominate the stripping. The theoretical curves fall off faster than the experimentally measured distributions, which show a tendency to level off in the region $\Theta > 140^\circ$. The insensitiveness of the stripping integral to the value of the cutoff radius parameter is demonstrated by numerical calculations.

INTRODUCTION

IN (d, p) reactions on heavy nuclei with low-energy deuterons the repulsive effect of the Coulomb field plays a dominant role, so that the effect of specifically nuclear interactions on the angular distribution of the protons is expected to be of minor importance. The theory of Coulomb stripping has been treated by Ter-Martirosian¹ and by Biedenharn *et al.*² Recent experimental measurements by Stokes³ of the angular distributions of the proton groups resulting from the bombardment of isotopes of Pb and Bi by deuterons with energies less than 10 Mev provide a test of the Coulomb stripping theory.⁴

ANGULAR DISTRIBUTION

The Coulomb stripping amplitude is given by the overlap integral of the (bound) neutron wave function and the Coulomb waves for proton and deuteron^{1,2}:

$$B^{Lm} = -(4\pi)^{-\frac{1}{2}} N_L (2\alpha)^{\frac{1}{2}} \int \psi_p^*(\mathbf{r}) Y_L^{m*}(\hat{r}) \times h_L^{(1)}(ik_n r) \psi_d(\mathbf{r}) d\mathbf{r}. \quad (1)$$

In this expression L = number of units of orbital angular momentum transferred by captured neutron, N_L = normalization constant, α = reciprocal radius of deuteron = $(ME_b/\hbar^2)^{\frac{1}{2}} = (4.32f)^{-1}$, $h_L^{(1)}$ = spherical Hankel function, Y_L^m = spherical harmonic.⁵ (The zero-range potential has been assumed for the deuteron.) The explicit

forms of the Coulomb waves are given by⁶

$$\begin{aligned} \psi_d &= \Gamma(1+i\eta_d) e^{-\frac{1}{2}\pi\eta_d} e^{i\mathbf{k}_d \cdot \mathbf{r}} \\ &\quad \times {}_1F_1[-i\eta_d, 1, i(k_d r - \mathbf{k}_d \cdot \mathbf{r})], \\ \psi_p^* &= \Gamma(1+i\eta_p) e^{-\frac{1}{2}\pi\eta_p} e^{-i\mathbf{k}_p \cdot \mathbf{r}} \\ &\quad \times {}_1F_1[-i\eta_p, 1, i(k_p r + \mathbf{k}_p \cdot \mathbf{r})]. \end{aligned} \quad (2)$$

k_n, k_p, k_d are the wave numbers of neutron, proton, and deuteron, respectively. η = Coulomb parameter = $Ze^2/\hbar v$. (v = relative velocity.)

Since the wave functions describing the relative motions of deuteron and proton decrease exponentially as $r \rightarrow 0$ (barrier effect), the important region for the evaluation of the stripping integral is $R \lesssim r$, where R = "cutoff radius." Numerical results reported here show that for η_p, η_d sufficiently large R can be taken greater than the range of specifically nuclear interactions. To be sure, the stripping process is itself caused by the nuclear forces, so that our statement means in effect that—aside from the stripping itself—the effect of nuclear forces on the deuteron and proton motion can be neglected for E small compared to the Coulomb barrier.⁷

NUMERICAL RESULTS AND COMPARISON WITH EXPERIMENT

In order to obtain theoretical angular distributions for comparison with the data of Stokes,³ the square of the magnitude of the stripping integral was calculated numerically. In the case where the neutron is captured with angular momentum zero, it was found convenient to write the integral in the form $\int_{\infty}^0 = \int_0^{\infty} - \int_0^R$; the \int_0^{∞} can be expressed in terms of the hypergeometric function⁸:

$$\begin{aligned} B^{00} &= (2\pi)^{-1} N_0 (2\alpha)^{\frac{1}{2}} \Gamma(1+i\eta_d) \Gamma(1+i\eta_p) e^{-\frac{1}{2}\pi(\eta_d+\eta_p)} \\ &\quad \times k_n^{-1} (k_n^2 + q^2)^{-1-i\eta_p-i\eta_d} (2ik_p k_n - k_n^2 + k_p^2 - k_d^2)^{i\eta_p} \\ &\quad \times (-k_n^2 + k_d^2 - k_p^2 + 2ik_n k_d)^{i\eta_d} \\ &\quad \times {}_2F_1(-i\eta_p, -i\eta_d, 1, x), \end{aligned} \quad (3)$$

⁶ L. I. Schiff, *Quantum Mechanics* (McGraw-Hill Book Company, Inc., New York, 1949), pp. 117–119.

⁷ Cf. reference 11.

⁸ Note that misprints in Eq. (5) of reference 2 have been corrected here. Other *errata* occur on p. 385 of reference 2. Thus, the exponent of the $(1-x)$ term in Eq. (7) should be $i(\eta_p + \eta_d)/2$; the expression for g [Eq. (8)] should include a factor $\frac{1}{2}$; the expression for a^2 [Eq. (11)] should be multiplied by $\frac{1}{2} k_p k_d$.

* Work performed under the auspices of U. S. Atomic Energy Commission.

† Permanent address: Department of Physics, Duke University, Durham, North Carolina.

¹ K. A. Ter-Martirosian, J. Exptl. Theoret. Phys. (USSR) **29**, 713 (1955); Soviet Phys.—JETP **2**, 620 (1956).

² L. C. Biedenharn, K. Boyer, and M. Goldstein, Phys. Rev. **104**, 383 (1956).

³ R. H. Stokes, Phys. Rev. **121**, 613 (1961).

⁴ The authors have been informed that measurements with a multiple-gap spectrograph of the angular distributions of the protons following bombardment of Bi²⁰⁹ by low-energy deuterons are in progress at M.I.T. (J. R. Erskine, unpublished.) See Fig. 5.

⁵ The caret symbol is used to denote a unit vector, i.e., a direction.

with

$$q^2 = k_d^2 + k_p^2 - 2\mathbf{k}_d \cdot \mathbf{k}_p,$$

$$x = \frac{4k_p k_d \sin^2(\Theta/2)}{k_d^2 + k_p^2 + k_n^2 - 2k_p k_d},$$

$$\Theta = \cos^{-1}(\hat{k}_d \cdot \hat{k}_p).$$

The form (3) was used to evaluate \int_0^∞ ; for the evaluation of \int_0^R the Coulomb waves are expanded in partial waves⁶:

$$e^{i\mathbf{k}_d \cdot \mathbf{r}} {}_1F_1[-i\eta_d, 1, i(k_d r - \mathbf{k}_d \cdot \mathbf{r})]$$

$$= [\Gamma(1+i\eta_d)]^{-1} \sum_l e^{i\sigma_l + i(\pi/2)l + (\pi/2)\eta_d}$$

$$\times (2l+1)(k_d r)^{-1} F_l(\eta_d, k_d r) P_l(\hat{k}_d \cdot \hat{r}),$$

and a similar expression for ψ_p . F_l is the Coulomb function regular at the origin. The integration over angles can be carried out making use of the addition theorem

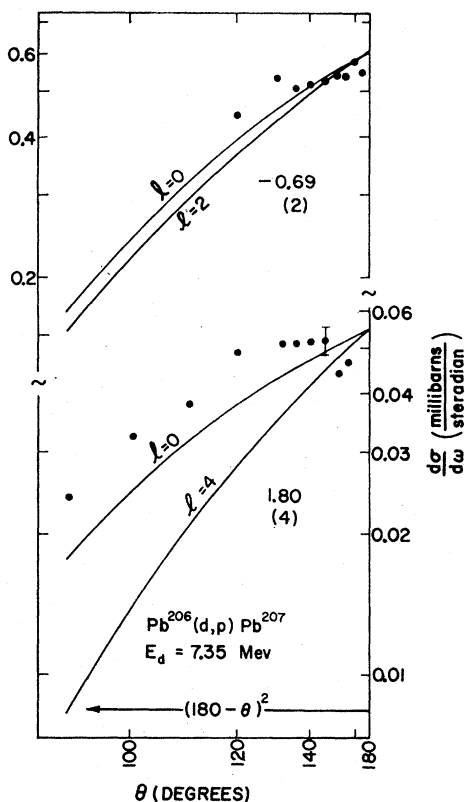


FIG. 1. Theoretical angular distributions for $\text{Pb}^{206}(d,p)\text{Pb}^{207}$. $E_d = 7.35$ Mev. Also shown are the experimental points of Stokes (reference 3). The curves are labeled by the Q value (Mev); the value of l_n = number of units of orbital angular momentum transferred by the captured neutron, deduced by Holm, Burwell, and Miller (reference 13) on the basis of identification of corresponding shell-model states in the isotopes Pb^{207} , Pb^{209} , Bi^{210} , is given in parentheses. The normalization of the computed angular distributions is arbitrary; The curves do not represent a "best fit" to the experimental points.

$[2(k_p - \frac{1}{2}k_d)^2 + k_0^2]$. These *errata* account for the difference noticed by Stokes in his paper. A correction was sent too late to Stokes to be included in his paper.

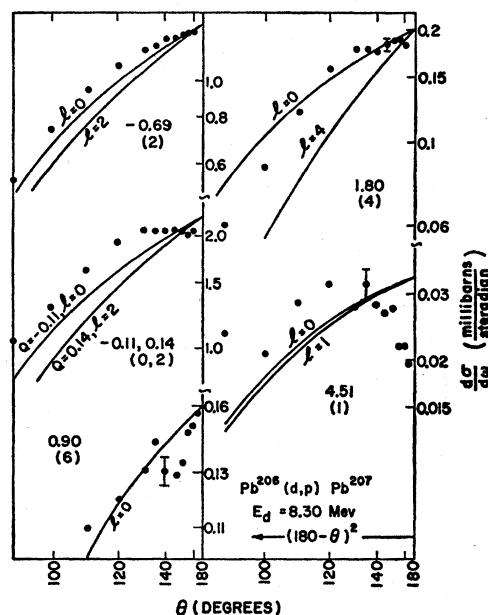


FIG. 2. Theoretical angular distributions for $\text{Pb}^{206}(d,p)\text{Pb}^{207}$. $E_d = 8.30$ Mev. Also shown are the experimental points of Stokes (reference 3).

for the Legendre polynomials; the result is

$$\int d\Omega_r e^{i(\mathbf{k}_d \cdot \mathbf{r} - \mathbf{k}_p \cdot \mathbf{r})} {}_1F_1[-i\eta_d, 1, i(k_d r - \mathbf{k}_d \cdot \mathbf{r})]$$

$$\times {}_1F_1[-i\eta_p, 1, i(k_p r + \mathbf{k}_p \cdot \mathbf{r})]$$

$$= \frac{4\pi e^{\frac{3}{2}\pi(\eta_d + \eta_p)}}{k_d k_p r^2 \Gamma(1+i\eta_d) \Gamma(1+i\eta_p)}$$

$$\times \sum_l (2l+1) F_l(d) F_l(p) e^{i[\sigma_l(\eta_d) + \sigma_l(\eta_p)]} P_l(\hat{k}_d \cdot \hat{k}_p).$$

It was found that 6 to 10 partial waves gave sufficient accuracy for the numerical evaluation of \int_0^R . Since an expression equivalent to (3) has not been found for the case L different from zero, the \int_0^∞ must be evaluated by making use of the partial wave expansions in this case.⁹

The theoretical angular distributions are compared with the data of Stokes³ in Figs. 1-4.¹⁰ The calculated angular distributions employed the value $R = 7$ f for the cutoff radius: The results shown in Figs. 6-8 demonstrate the insensitiveness of the stripping overlap integral to the value of R [for values of $R \lesssim (\frac{4}{3})$ mini-

⁹ A general machine code for stripping reactions, developed by W. Tobocman and W. Gibbs and adapted for the Los Alamos machines by L. S. Rodberg and Blair Swartz, was kindly made available for purposes of testing the $L=0$ code by Dr. William Gibbs and Dr. Blair Swartz. The results reported here for $L > 0$ were obtained by adapting the TGRS code to the case of pure Coulomb stripping. A machine program for the regular Coulomb function was furnished by Dr. George Baker. The machine program for the ${}_2F_1$ function was written by Dr. Max Goldstein.

¹⁰ Figure 5 is a similar comparison with unpublished data of Erskine. (See reference 4.) The authors are grateful to Mr. Erskine for permission to make use of his preliminary results.

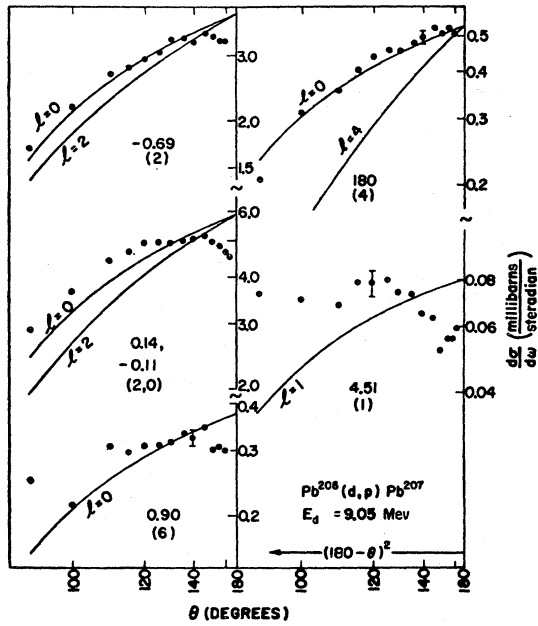


FIG. 3. Theoretical angular distributions for $Pb^{206}(d,p)Pb^{207}$. $E_d=9.05$ Mev. Also shown are the experimental points of Stokes (reference 3).

num of $(\eta_p/k_p, \eta_d/k_d)$, and establish the validity of the assumption neglecting the contribution of the region $r < R$, which includes the "interior" of the residual nucleus.¹¹ The "barrier height" for deuterons on Bi

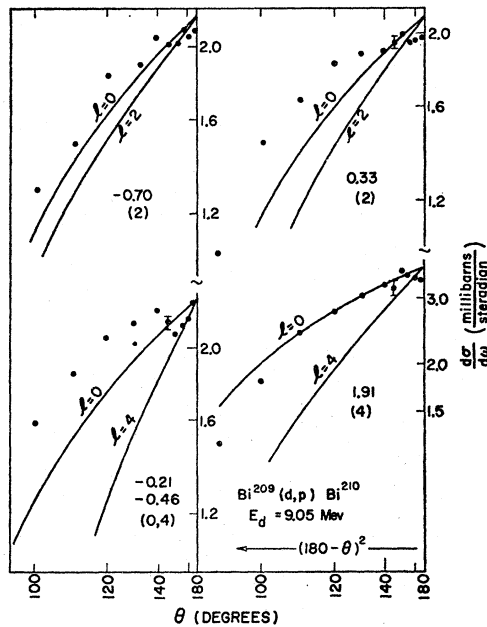


FIG. 4. Theoretical angular distributions for $Bi^{209}(d,p)Bi^{210}$. $E_d=9.05$ Mev. Also shown are the experimental points of Stokes (reference 3).

¹¹ Using the TGRS code, optical-model calculations were made for the case $E_d=7.35$ Mev, $Q=1.8$ Mev, to estimate the effect of

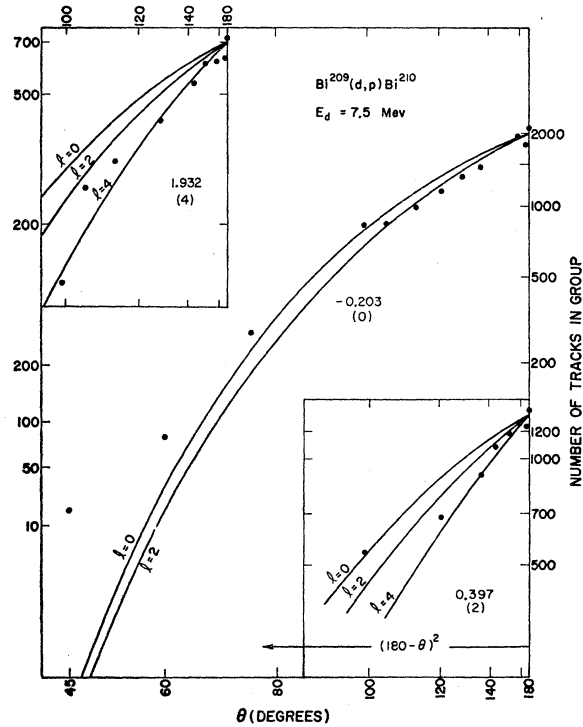


FIG. 5. Theoretical angular distributions for $Bi^{209}(d,p)Bi^{210}$. $E_d=7.5$ Mev. Also shown are the experimental points of Erskine (reference 4).

is 17.1 Mev, corresponding to an assumed nuclear radius $= 7$ f.

Both theoretical and experimental angular distributions (Figs. 1-5) show the same peaking in the backwards direction, characteristic where Coulomb effects dominate the stripping. In general, the theoretical curves fall off faster than the experimentally measured distributions, which also show a tendency to level off in the region $\Theta > 140^\circ$. (The normalization of the computed angular distributions is arbitrary: The curves do not represent a "best fit" to the experimental points.) Both references 1 and 2 show that the theoretical angular distribution becomes approximately of Gaussian form peaked at 180° in the limit of large η . The coordinate scales for Figs. 1-5 are arranged so that such a distribution would be represented by a straight line.

The approximations made in the theory as developed in references 1 and 2 may be summarized as follows: (1) use of first-order perturbation theory; (2) neglect of effects of polarizability and dissociation of deuteron; (3) neglect of D -state component of deuteron ground state and tensor neutron-proton interaction; (4) neglect

nuclear forces on the stripping angular distribution. Reasonable values of the optical potential parameters cause only small changes in the asymptotic phase shifts of the Coulomb waves for deuteron and proton; the calculated elastic scattering and stripping differential cross sections deviate only slightly from those predicted by the Rutherford and Butler-Coulomb theories.

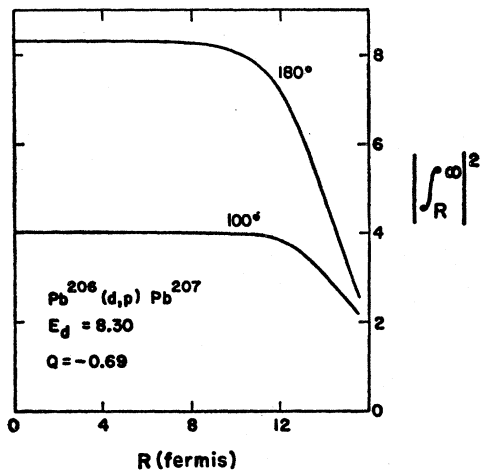


FIG. 6. Results of numerical evaluation of the ($l_n=0$) Coulomb stripping overlap integral for different values of the cutoff radius parameter R . The values of the other parameters are: $\eta_d=6.3$, $\eta_p=4.7$, $k_d=0.88$ f $^{-1}$, $k_p=0.60$ f $^{-1}$, $k_n=0.57$ f $^{-1}$, $\bar{r}_d=14.3$ f, $\bar{r}_p=15.7$ f. (\bar{r} =classical distance of closest approach for $l=0$ particle= $2\eta/k$.)

of specifically nuclear interactions; (5) neglect of spin-orbit interactions; (6) neglect of contribution of "compound nucleus" processes. Of these approximations,

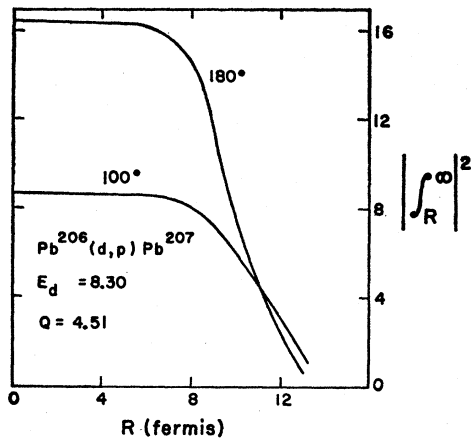


FIG. 7. Results of numerical evaluation of the ($l_n=0$) Coulomb stripping overlap integral for different values of the cutoff radius parameter R . The values of the other parameters are: $\eta_d=6.3$, $\eta_p=3.6$, $k_d=0.88$ f $^{-1}$, $k_p=0.78$ f $^{-1}$, $k_n=0.57$ f $^{-1}$, $\bar{r}_d=14.3$ f, $\bar{r}_p=9.2$ f.

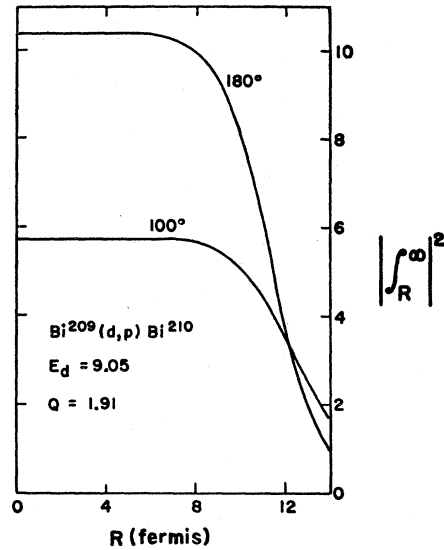


FIG. 8. Results of numerical evaluation of the ($l_n=0$) Coulomb stripping overlap integral for different values of the cutoff radius parameter R . The values of the other parameters are: $\eta_d=6.1$, $\eta_p=3.9$, $k_d=0.92$ f $^{-1}$, $k_p=0.72$ f $^{-1}$, $k_n=0.44$ f $^{-1}$, $\bar{r}_d=13.3$ f, $\bar{r}_p=10.8$ f.

undoubtedly the most severe is the neglect of polarizability and dissociation of the deuteron. Our purpose here was to show explicitly that the approximations in the Butler-Coulomb theory for the stripping angular distribution are justified in the region $E_d \lesssim 10$ Mev on nuclei with $Z \approx 80$.^{12,13}

ACKNOWLEDGMENTS

The authors have benefited from discussion with Dr. T. A. Griffy. The assistance of Mrs. Phyllis Heyman and Mrs. Beatrice Hindman in the preparation of the manuscript is acknowledged.

¹² It is remarkable, however, that neutron widths determined by making use of the absolute differential cross-section measurements of Stokes and the values of L deduced by Holm *et al.* (reference 13) are larger than single-particle values by factors ranging from 1.5 to 10, with one exception, viz, the level in Pb^{207} corresponding to $Q=4.51$ Mev.

¹³ G. B. Holm, J. R. Burwell, and D. W. Miller, Phys. Rev. 118, 1247 (1960).